LABORATORI NAZIONALI DI FRASCATI
SIS-Pubblicazioni

Searching for $K_L \to \pi^0 \nu \bar{\nu}$ at a Φ–factory

F. Bossi, G. Colangelo and G. Isidori

INFN, Laboratori Nazionali di Frascati,
I–00044 Frascati, Italy

Abstract

The perspectives of a search for the rare decay $K_L \to \pi^0 \nu \bar{\nu}$ at a Φ–factory are discussed. After a general analysis, we focus on the realistic case of KLOE and DAΦNE, showing that limits of the order of 10^{-9} on BR($K_L \to \pi^0 \nu \bar{\nu}$) are achievable in the next few years. We also discuss the theoretical implications of this kind of measurements.

Submitted to
The European Journal of Phys. C

1 Introduction

Flavor–changing neutral–current kaon decays provide a fundamental probe to investigate the flavor structure of electroweak interactions [1,2]. Among them, $K \to \pi\nu\bar{\nu}$ transitions can be considered the "gold–plated" channels because of their freedom from long–distance uncertainties [3–7]. A measurement of the $K \to \pi\nu\bar{\nu}$ decay widths would provide unique informations on fundamental parameters of the Standard Model, and possibly also on the physics beyond it, as has been recently emphasized in [8–11]. In recent years an important experimental challenge has been undertaken to observe such transitions, and very recently preliminary evidence for $K^+ \to \pi^+\nu\bar{\nu}$ was found [12]. Despite this success, the experimental difficulties in the neutral channels ($K_{L,S} \to \pi^0\nu\bar{\nu}$) are still far form being solved.

Although the signature of the $K_L \to \pi^0\nu\bar{\nu}$ decay looks at first straightforward (two photons whose invariant mass equals that of a π^0 and nothing else), the problem of backgrounds rejection has so far proven to be very difficult to handle, resulting in rather poor limits on the corresponding branching ratio. In fact, the decay channels of the K_L^0 into 2 or 3 π^0's have branching ratios several orders of magnitude larger than the one expected for the signal, requiring, therefore, a very high photon detection capability. This is particularly important in view of the practical impossibility to completely reconstruct the decay kinematics at hadron machines, where all the searches for $K_L \to \pi^0\nu\bar{\nu}$ have been performed thus far. Moreover, at these machines, kaon beams are accompanied by unwanted neutral–hadron halos, which can fake the signal either by interaction with the residual gas in the decay volume or via decays such as $\Lambda \to \pi^0 n$.

With the present paper we want to draw attention to the fact that many of the problems listed above have a natural solution if the search is performed at a ϕ–factory. The K_L beam available at a ϕ–factory is *monochromatic*, which allows the complete reconstruction of the decay kinematics, greatly helping in the rejection of the most dangerous physics background i.e. $K_L \to \pi^0\pi^0$. Moreover, since it is a *tagged* beam, it is also free from the background due to accidentals which can mimic the signal.

The paper is organized as follows. In the next section we briefly introduce the theoretical framework needed to describe this decay, and discuss the implications of a measurement of the $K \to \pi\nu\bar{\nu}$ decay widths. In section 3 we describe the present experimental status on $K_L \to \pi^0\nu\bar{\nu}$ searches and the prospects for future measurements. Section 4 is devoted to the study of the feasibility of this measurement at a ϕ–factory, with special attention to what can be obtained, in a short time frame, at facilities which are at present in the commissioning phase. Our conclusion are then summarized in the final section.

2 Theoretical overview

Within the Standard Model, $K \to \pi\nu\bar{\nu}$ transitions can be described by means of the following effective four–fermion Hamiltonian

$$\mathcal{H}_{\text{eff}} = \frac{\alpha G_F}{2\sqrt{2}\pi \sin^2 \Theta_W} \sum_{l=e,\mu,\tau} C^l \, \bar{s}\gamma^\mu(1-\gamma_5)d \, \bar{\nu}_l\gamma_\mu(1-\gamma_5)\nu_l \; + \; \text{h.c.} \qquad (1)$$

The Wilson Coefficients C^l have been calculated by Buchalla and Buras including next–to–leading order QCD corrections [4] and, recently, also $O(G_F^2 m_t^4)$ effects [5]. Neglecting the latter, which represent at most a few percent correction, we can write [4]

$$C^l = \lambda_c X_{NL}^l + \lambda_t X(m_t^2/M_W^2) \, , \qquad (2)$$

where $\lambda_q = V_{qs}^* V_{qd}$, V_{ij} denotes the Cabibbo–Kobayashi–Maskawa (CKM) [13] matrix elements and the X functions can be found in [4] (see also [14]). Numerically, $X_{NL}^l \sim 10^{-3}$ and $X(m_t^2/M_W^2) \simeq 1.5$; thus charm and top contributions to the real part of C^l are comparable since $\text{Re}(\lambda_c)/\text{Re}(\lambda_t) \sim \mathcal{O}(10^{-3})$, while the top contribution dominates the imaginary part because $\text{Im}(\lambda_c)/\text{Im}(\lambda_t) \sim \mathcal{O}(1)$.

The matrix elements of the Hamiltonian (1) between kaon and pion states are well known since they are related by isospin symmetry to those relevant for the corresponding (charged current) semileptonic decays. Neglecting isospin breaking effects we can write for the case of our interest

$$\left| \sqrt{2}\langle \pi^0|\bar{s}\gamma^\mu d|K^0\rangle \right| = \left| \sqrt{2}\langle \pi^0|\bar{d}\gamma^\mu s|\bar{K}^0\rangle \right| =$$
$$\langle \pi^+(p_\pi)|\bar{s}\gamma^\mu d|K^+(p_K)\rangle = f_+(q^2)(p_\pi^\mu + p_K^\mu) + \mathcal{O}(q^\mu = p_K^\mu - p_\pi^\mu) \, , \qquad (3)$$

where

$$f_+(q^2) = 1 + \lambda\frac{q^2}{M_{\pi+}^2} \qquad \text{and} \qquad \lambda = (0.030 \pm 0.002) \, . \qquad (4)$$

Thus the three decay modes have the same spectrum and only differ by a normalization factor. In the charged case we find

$$\frac{\mathrm{d}\Gamma(K^+ \to \pi^+\nu_l\bar{\nu}_l)}{\mathrm{d}E_\pi} = \frac{\alpha^2 G_F^2 |C^l|^2 M_K}{48\pi^5 \sin^4 \Theta_W} \left| f_+(q^2) \right|^2 (E_\pi^2 - M_\pi^2)^{3/2} \, , \qquad (5)$$

where

$$M_\pi \leq E_\pi \leq E_\pi^{\text{max}} = \frac{M_K}{2}\left(1 + \frac{M_\pi^2}{M_K^2}\right) \qquad \text{and} \qquad q^2 = M_K^2 + M_\pi^2 - 2M_K E_\pi \, . \qquad (6)$$

The relative phase between the neutral matrix elements in (3) depends on the phase convention for $|K^0\rangle$ and $|\bar{K}^0\rangle$ states. Assuming the matrix elements to be real and imposing $CP|K^0\rangle = |\bar{K}^0\rangle$ leads to $\langle\pi^0|\bar{s}\gamma^\mu d|K^0\rangle = \langle\pi^0|\bar{d}\gamma^\mu s|\bar{K}^0\rangle$. Then defining as usual

$$|K_{L,S}\rangle = \frac{1}{\sqrt{2(1+|\epsilon|^2)}}\left((1+\epsilon)|K^0\rangle \mp (1-\epsilon)|\bar{K}^0\rangle\right) \tag{7}$$

and neglecting the suppressed $\mathcal{O}(\epsilon)$ terms[1] leads to

$$\frac{A(K_S \to \pi^0\nu_l\bar{\nu}_l)}{|A(K^+ \to \pi^+\nu_l\bar{\nu}_l)|} = \frac{\mathrm{Re}C^l}{|C^l|} \simeq \frac{\rho_0^l - \bar{\rho}}{\sqrt{(\sigma\bar{\eta})^2 + (\bar{\rho}-\rho_0^l)^2}}\, , \tag{8}$$

$$\frac{A(K_L \to \pi^0\nu_l\bar{\nu}_l)}{|A(K^+ \to \pi^+\nu_l\bar{\nu}_l)|} = \frac{i\mathrm{Im}C^l}{|C^l|} \simeq -\frac{i\sigma\bar{\eta}}{\sqrt{(\sigma\bar{\eta})^2 + (\bar{\rho}-\rho_0^l)^2}}\, . \tag{9}$$

Here we have used the Wolfenstein parametrization of the CKM matrix [17] in its modified version (first introduced by [15] and then redefined in [16]):

$$\lambda_t = -\sigma^{-1/2}A^2\lambda^5(1-\bar{\rho}-i\sigma\bar{\eta}) \doteq |\lambda_t|e^{i\beta}\, ,$$
$$\mathrm{Re}(\lambda_c) = -\lambda\sigma^{-1/2}\, ,$$
$$\mathrm{Im}(\lambda_c) = -\mathrm{Im}(\lambda_t)\, , \tag{10}$$

where[2] $\lambda = |V_{us}|$, $(\rho + i\eta) = V_{ub}^*/(V_{us}V_{cb})$, $\sigma^{-1/2} = (1 - \lambda^2/2)$, $\bar{\rho} = \sigma^{-1/2}\rho$ and $\bar{\eta} = \sigma^{-1/2}\eta$. The dominant contribution to all the amplitudes is independent of the lepton flavour and is proportional to the λ_t term in (2). The charm contamination is totally negligible in the K_L decay, but induces the largest theoretical uncertainty in the evaluation of the real part of C^l. This contribution is parametrized by

$$\rho_0^l - 1 = \frac{X_{NL}^l}{A^2\lambda^4 X(m_t^2/M_W^2)} \lesssim 0.3 \quad [14]\, . \tag{11}$$

For later convenience we also recall that the latest numerical analysis of the CKM matrix yields [14]:

$$\lambda = 0.2205 \pm 0.0018\, , \quad |\lambda_t| = (3.5 \pm 0.5) \times 10^{-4}\, , \quad \beta \sim (10 \div 30)^\circ\, . \tag{12}$$

We remark that since the $\pi^0\nu_l\bar{\nu}_l$ state produced by $\mathcal{H}_{\mathrm{eff}}$ is CP–even, the $K_L \to \pi^0\nu_l\bar{\nu}_l$ amplitude has to vanish in the limit of exact CP symmetry, as it is apparent from Eq. (9).

---

[1] In our phase convention $\mathrm{Im}\,\epsilon \sim \mathrm{Re}\,\epsilon \sim \mathcal{O}(10^{-3})$.

[2] For simplicity we use a definition of λ, ρ and η which is not exactly that given in [16]. On the other hand, the relative difference is of $\mathcal{O}(\lambda^6)$ which is far beyond the accuracy we need.

In principle there is also a long–distance contribution, generated by light quark rescattering, that can be calculated in the framework of Chiral Perturbation Theory. This amounts to a few percent correction to ρ_0^l [6] and, being much smaller than the scale uncertainty of the charm contribution, can be safely neglected. In passing, we note that long–distance effects vanish at $O(p^2)$ only if exact nonet symmetry is assumed, as correctly stated in [6] (and in contrast to what has been claimed in [18]).

Eqs. (8-9) imply an interesting relation among the three the decay widths[3]

$$\Gamma(K_L \to \pi^0\bar{\nu}\nu) + \Gamma(K_S \to \pi^0\bar{\nu}\nu) = \Gamma(K^+ \to \pi^+\bar{\nu}\nu) \ . \tag{13}$$

This is a direct consequence of (3) and indeed receives small corrections due to isospin–breaking terms, which have been evaluated in [7]. These are generated by the mass difference $m_d - m_u$ and by electromagnetic effects.

The expressions for the branching ratios of the three decay transitions $K \to \pi\nu\bar{\nu}$ are as follows:

$$BR(K^+ \to \pi^+\nu\bar{\nu}) = \kappa_+ \frac{1}{3} \sum_l \left| C^l/\lambda^5 \right|^2 \ ,$$

$$BR(K_L \to \pi^0\nu\bar{\nu}) = \kappa_L \frac{1}{3} \sum_l \left[\mathrm{Im}(C^l/\lambda^5) \right]^2 \ , \tag{14}$$

$$BR(K_S \to \pi^0\nu\bar{\nu}) = \kappa_S \frac{1}{3} \sum_l \left[\mathrm{Re}(C^l/\lambda^5) \right]^2 \ ,$$

$$\tag{15}$$

where

$$\kappa_+ = r_{K+} \frac{3\alpha^2 BR(K^+ \to \pi^0 e^+\nu)}{2\pi^2 \sin^4\Theta_W} \lambda^8 = 4.11 \times 10^{-11} \ . \tag{16}$$

This number has been obtained using $\alpha = 1/129$, $\sin^2\Theta_W = 0.23$, $BR(K^+ \to \pi^0 e^+\nu) = 4.82 \times 10^{-2}$, as in [14], and $r_{K+} = 0.9$ which summarizes isospin breaking corrections [7]. The factor κ_+ gives the order of magnitude one should expect for $BR(K^+ \to \pi^+\nu\bar{\nu})$, since C^l/λ^5 is roughly a number of order one within the Standard Model. A detailed numerical analysis for this last term using present constraints on the CKM matrix leads to [14]:

$$BR(K^+ \to \pi^+\nu\bar{\nu})_{\mathrm{SM}} = (8.0 \pm 1.5) \times 10^{-11} \ . \tag{17}$$

The corresponding κ factors for the neutral kaons are defined as

$$\kappa_{L,S} = \kappa_+ \frac{\tau_{K_{L,S}}}{\tau_{K+}} \frac{r_{K^0}}{r_{K+}} \ , \tag{18}$$

---

[3] When the lepton flavor is not explicitly indicated, the sum over neutrino's families is understood.

where $r_{K^0} = 0.94$ has been calculated in [7], and yields [14]:

$$BR(K_L \to \pi^0 \nu \bar\nu)_{\text{SM}} = (2.6 \pm 0.9) \times 10^{-11} \ , \tag{19}$$

while for the K_S the suppression due to the very short lifetime leads to a branching ratio of order 10^{-13}.

2.1 $K \to \pi \nu \bar\nu$ beyond the Standard Model

In most New Physics models $K \to \pi \nu \bar\nu$ transitions are still described by the effective Hamiltonian (1), with appropriate Wilson coefficients $C^l_{NP} \neq C^l_{SM}$. This is the case for "typical" supersymmetric models, see e.g. [10,11], but also for SM extensions with strong dynamics at the electroweak scale [9]. Within this framework, a convenient parameterization of the Wilson coefficient is given by [11]

$$\begin{aligned} C^l_{NP} &= \lambda_c X^l_{NL} + e^{i\theta_K} r_K \lambda_t X(m_t^2/M_W^2) \\ &= \lambda_c X^l_{NL} + e^{i(\theta_K + \beta)} r_K |\lambda_t| X(m_t^2/M_W^2) \ , \end{aligned} \tag{20}$$

with r_K real and positive and $-\pi < \theta_K < \pi$ (the SM case is recovered for $r_K = 1$ and $\theta_K = 0$). In both supersymmetric and strong–dynamics scenarios, the natural size of the parameter r_K is $0.5 \lesssim r_K \lesssim 2$, implying small deviations of $BR(K^+ \to \pi^+ \nu \bar\nu)$ from its SM value. However, even for $r_K \sim 2$ a large enhancement of $BR(K_L \to \pi^0 \nu \bar\nu)$ is possible provided the *new–physics phase* θ_K is such that $|\theta_K + \beta| \sim \pi/2$. This possibility is not particularly likely but, at least in some supersymmetric scenarios, still not excluded by data in other channels [10,11].

Taking a more general point of view, Grossman and Nir [8] have shown that the situation is different if one considers models with non–vanishing neutrino masses and/or lepton–flavor violations. In this case one can write different kinds of dimension–six operators, like $\bar s d \bar\nu_l \nu_l$ or even $\bar s d \bar\nu_l \nu_m$. Furthermore, if lepton flavor is violated $K_L \to \pi^0 \nu \bar\nu$ can receive also CP–conserving contributions [8].

Interestingly enough, in all these cases the relation (13) is still valid (up to small isospin breaking corrections). This is because any $s \to d$ two–quark operator carries isospin $\Delta I = 1/2$ and thus obeys the isospin relation $|\sqrt{2} \langle \pi^0 | O_{\bar s d} | K^0 \rangle| = |\langle \pi^+ | O_{\bar s d} | K^+ \rangle|$. The only way to avoid this constraint is to consider a $\Delta I = 3/2$ operator, that is at least dimension nine for the $s \to d \nu \bar\nu$ transition. Neglecting the effect of this presumably much suppressed operator, from Eq. (13) one can derive a model–independent bound [8] on $BR(K_{L,S} \to \pi^0 \nu \bar\nu)$ in terms of the measured $BR(K^+ \to \pi^+ \nu \bar\nu)$ [12]

$$BR(K_L \to \pi^0 \nu \bar\nu) \ < \ \frac{\tau_{K_L}}{\tau_{K^+}} BR(K^+ \to \pi^+ \nu \bar\nu) \left[1 + \mathcal{O}\left(\frac{m_u - m_d}{m_s}\right) \right] \lesssim 5 \times 10^{-9} \ , \tag{21}$$

$$BR(K_S \to \pi^0 \nu\bar{\nu}) \quad < \quad \frac{\tau_{K_S}}{\tau_{K^+}} BR(K^+ \to \pi^+ \nu\bar{\nu}) \left[1 + \mathcal{O}\left(\frac{m_u - m_d}{m_s} \right) \right] \lesssim 9 \times 10^{-12} \; . \quad (22)$$

Any experimental limit on $BR(K_{L,S} \to \pi^0 \nu\bar{\nu})$ below these values carries a non–trivial dynamical information on the structure of the $s \to d\nu\bar{\nu}$ amplitude.

In models where $K \to \pi\nu\bar{\nu}$ transitions are described by the effective Hamiltonian (1), a measurement of $BR(K_L \to \pi^0 \nu\bar{\nu})$ (or $BR(K_S \to \pi^0 \nu\bar{\nu})$) fixes $|\mathrm{Im}C|$ (or $|\mathrm{Re}C|$), whereas $BR(K^+ \to \pi^+ \nu\bar{\nu})$ determines $|C|$ (here, for simplicity, we are assuming lepton universality). Thus C can be fixed up to a four–fold ambiguity. In order to disentangle non SM effects it could be important to resolve this ambiguity (see e.g. the discussion of [19]). Even if present and foreseen facilities do not allow for this possibility, we find it amusing to note that this could be done in principle in a very high luminosity Φ–factory, looking at $K_{L,S} \to \pi^0 \nu\bar{\nu}$ interference. Here, analogously to the double final state $|\pi^+ \pi^-, \pi^0 \pi^0\rangle$ analyzed for the measurement of ϵ'/ϵ, one could study the time–difference distribution [20] of $|\phi\rangle \to |\pi^+ \pi^-, \pi^0 \nu\bar{\nu}\rangle$. This is given by

$$I(\pi^0 \nu\bar{\nu}, \pi^+ \pi^-; t) \propto \frac{e^{-\Gamma|t|}}{2\Gamma} \left\{ |\lambda_{\nu\bar{\nu}}|^2 e^{-\frac{\Delta\Gamma}{2}t} + |\eta_{+-}|^2 e^{+\frac{\Delta\Gamma}{2}t} - 2\mathrm{Re}\left(\eta_{+-}^* \lambda_{\nu\bar{\nu}} e^{i\Delta m t} \right) \right\} \; , \quad (23)$$

where $t = t_{\pi^+ \pi^-} - t_{\pi^0 \nu\bar{\nu}}$, $\Gamma = (\Gamma_S + \Gamma_L)/2$, $\Delta m = m_L - m_S$, $\Delta\Gamma = \Gamma_S - \Gamma_L$, and

$$\eta_{+-} = \frac{A(K_L \to \pi^+ \pi^-)}{A(K_S \to \pi^+ \pi^-)} \; , \quad \lambda_{\nu\bar{\nu}} = \frac{A(K_L \to \pi^0 \nu\bar{\nu})}{A(K_S \to \pi^0 \nu\bar{\nu})} \; . \quad (24)$$

Thus a measurement of the interference term would lead to an unambiguous determination of the sign of $\lambda = i \, \mathrm{Im} \, C/\mathrm{Re} \, C + \mathcal{O}(\epsilon)$.

3   Present Experimental Status and Prospects

At present, the best published limit for the $K_L \to \pi^0 \nu\bar{\nu}$ decay is 5.8×10^{-5} (90% C.L.), obtained by the FNAL experiment E799-I [21]. Recently, the KTEV Collaboration has presented a preliminary result, giving an upper limit on the branching ratio of 1.8×10^{-6} (90% C.L.) [22]. The same Collaboration aims at reaching in 1999 a single event sensitivity (that we will precisely define below) of 3×10^{-9}.

Sensitivities which should allow a positive measurement of the branching ratio (assuming the Standard Model value) are the goal of three dedicated experiments which have been recently proposed. The first should run at the new 50 GeV high–intensity machine in KEK [23]; the second is the KAMI experiment at FNAL, essentially an upgraded continuation of the KTEV experiment [22]; finally, there is the BNL proposal [24], whose approach is the closest to the one discussed in the present paper. In fact, the BNL group proposes to execute the experiment on a micro–bunched, low–momentum (~ 700 MeV) kaon beam,

with the purpose of measuring the momentum of the decaying K_L with a time–of–flight technique, allowing the complete reconstruction of the decay kinematics. The advantages of this experimental technique are similar to the ones discussed in the present paper, although the ϕ–factory environment is free from the uncertainties due to the presence of neutral halos in the kaon beam, typical of hadron machines.

However, the time scale for these experiments is such that the first results will not be available before year 2003, at best.

In the next section we will discuss the advantages of performing the measurement at a ϕ–factory, concentrating on the realistic case of the KLOE experiment [25–30] at DAΦNE [33]. We will show that results as good as the one expected from KTEV 99 can be obtained in a relatively short time.

4 $K_L \to \pi^0 \nu \bar{\nu}$ **at a** ϕ**–factory**

At a ϕ–factory, $\phi(1020)$ mesons are produced at rest by $e^+ e^-$ collisions. Due to C–parity conservation, they decay into a K_S–K_L pair with a branching ratio of 34.1% [31]. By observing the K_S decay into two charged pions, it is therefore possible to tag the presence of the K_L moving in the opposite direction with a ~ 110 MeV/c momentum, determined by the ϕ decay kinematics. Therefore the complete reconstruction of the kinematics of the subsequent K_L decay is allowed.

Presently the newly built ϕ–factory DAΦNE has begun commissioning in Frascati, with the peak luminosity of 5×10^{32} cm^{-2}s^{-1}. At this luminosity, as many as 10^{10} correlated K_S–K_L pair per year can be produced[4].

The KLOE detector at DAΦNE, whose roll–in is expected by mid 1998 [30], has been designed and built with the main purpose of determining the CP–violating parameter ϵ'/ϵ via the observation of the K_L decays into two charged or two neutral pions. A very high photon detection efficiency is one of the fundamental requirements for such a measurement; in particular great attention has been paid to the problem of minimizing the background from K_L decays into three neutral pions in which two photons escape detection [25,26]. For this reason KLOE is well suited also for the observation of the decay of interest in the present paper.

The detector consists of two main parts: a large cylindrical tracking chamber of 2 m radius and 3.7 m length, and a hermetic lead–scintillating fibers electromagnetic calorimeter (ECAL from now on). ECAL allows one to detect photons with energy down to 20 MeV and to measure their energy with a resolution of $\sigma_E = 4.5\% \times \sqrt{(E)}$ (E in GeV). In addition, ECAL allows the determination of the entry–point position of the photons with a

---

[4]Here and from now on, following HEP convention, we define one physics year to be equal to 10^7 s.

resolution of 3 cm and 1 cm for coordinates parallel and perpendicular to the scintillating fibers, respectively. Of great relevance is also the ability of the ECAL to determine the time of the photon's passage with a resolution of $\sigma_T = 60ps/\sqrt{(E)}$ (E in GeV).

In order to quantify the possible performance of such a detector, we have set up a simple Monte Carlo in which K_L–K_S pairs are generated from $\phi(1020)$ decays taking into account the correct energy and angular distributions; the K_L is then allowed to decay into 2 π^0's or $\pi^0\nu\bar{\nu}$, at a space point determined by its momentum and lifetime.

We have concentrated our attention on the problem of the rejection of the $K_L \to \pi^0\pi^0$ background which is the key issue for the success of the experiment (see section 4.3).

We will see that, although the main physical ideas and some of the conclusions of our paper are a generic consequence of the peculiar environment available at any ϕ–factory, ultimately the detector's parameters, such as geometrical acceptance and resolutions, become of decisive importance. We have therefore paid the maximum attention to the correct parametrization of such parameters trying, wherever possible, to check our conclusions with independent studies and official figures.

4.1 Description of the method

In our code the KLOE detector is implemented as a cylinder of 4 m diameter and 3.7 m length, hermetically closed at both ends by two endcaps. In the following, the cylinder axis is defined as the z axis.

One of the most important features of the KLOE detector is that it is almost perfectly hermetic to photons. There is however a small chance that a photon produced inside the detector is lost. The causes of the losses are the following:

1. There is a small region between the endcaps and the beam pipe where the detector has a physical hole: this can be schematically modeled by two squares of 50 cm side, one for each endcap.

2. The beam pipe inside the detector and the wall of the drift chamber can absorb photons. We have assigned a 2 % probability of absorption to photons intersecting the beam pipe or the internal walls of the drift chamber, implemented as a cylinder of 20 cm radius, with axis along the z direction.

3. Two sets of three low–β quadrupoles are inserted along the beam pipe inside the detector. In order to detect the photons that would have been lost hitting these quadrupoles, the latter are covered by special calorimeters (QCAL). However, the detection efficiency of QCAL is not expected to exceed 90-95 % [32]: in the program it has been assigned a 90% efficiency, independent on the photon's energy.
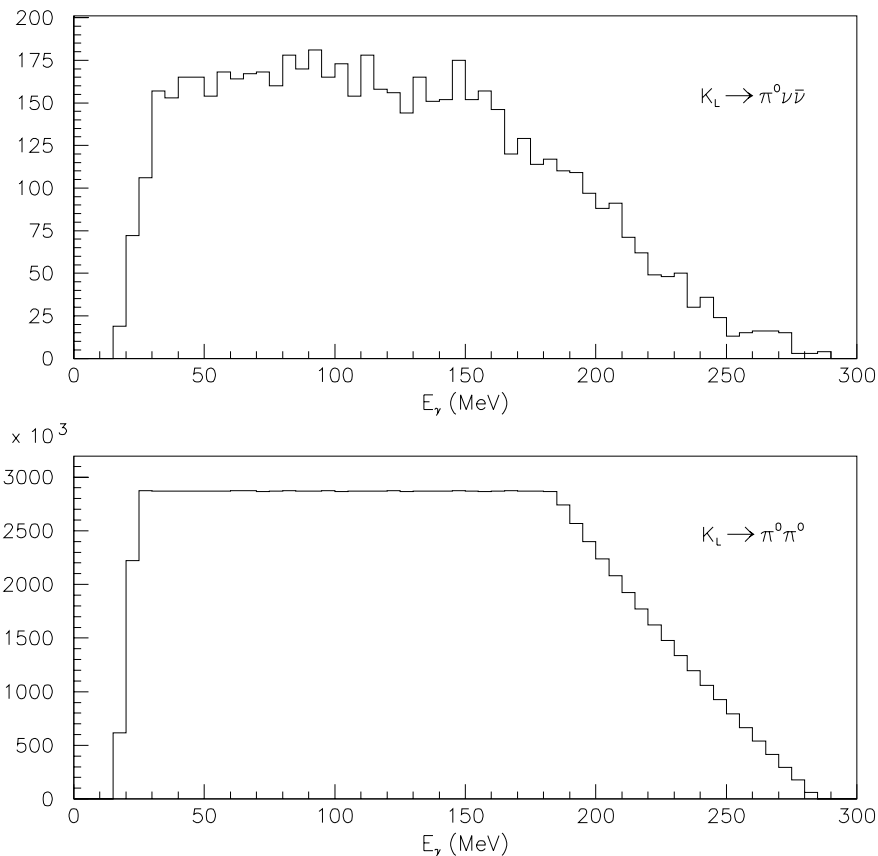
8

Figure 1: Energy distribution for photons produced by $K_L \rightarrow \pi^0 \nu \bar{\nu}$ (upper plot), and $K_L \rightarrow \pi^0 \pi^0$ events (lower plot)

4. Photon losses in ECAL due to some detection inefficiency are always possible. In particular, low energy photons can be lost because of several effects, including sampling fluctuations, photonuclear reactions, reconstruction inefficiencies. A detailed study of these effects goes well beyond the scope of the present paper. We have parametrized them by assigning a 70% detection probability to 20 MeV photons, linearly increasing up to 100% at 50 MeV. Photons with energy lower than 20 MeV were considered lost both for ECAL and QCAL. The energy distribution of the photons produced by $K_L \rightarrow \pi^0 \nu \bar{\nu}$ and $K_L \rightarrow \pi^0 \pi^0$ decays is shown in Figure 1.

The program computes the geometrical interception of the photons produced by the decays which happen inside KLOE and the calorimeter, and first of all decides whether the photons are lost or not. In order to check the reliability of our simulation, we have generated a sample of $K_L \rightarrow \pi^0 \pi^0 \pi^0$ events and compared the number of lost photons predicted by our program with the one predicted by the official KLOE Monte Carlo, GEANFI [25]. In this comparison only geometrical effects were taken into account, i.e. the fourth source

of photon losses discussed in the previous list was not considered. Decays happening inside a cylindrical fiducial volume defined by $-150 < z < 150$ and $40 < R < 180$ (z, R in cm) were studied. Inside this fiducial volume, GEANFI predicted a $0.83 \pm 0.02\%$ loss for photons, while our simulation gave $1.44 \pm 0.01\%$. The relative population of photons reaching the different parts of the detector were in agreement; our simulations turned out to be only slightly pessimistic in the prediction of photon losses on the beam–pipe or on the internal wall of the drift chamber. This result gave us confidence that our simplified Monte Carlo well reproduces the main features of the KLOE detector, as far as photon detection is concerned.

Once two photons reach the active part of the detector, they can be paired and their invariant mass can be computed. Here, detector's resolutions play a crucial role. For the energy and position resolutions of ECAL we have used the previously quoted figures. We have assigned a photon–energy resolution of $\sigma_E = 40\%$ to QCAL, independent of the photon's energy, while keeping the same spatial resolution used for those hitting ECAL.

The last piece of experimental information needed for the complete reconstruction of the K_L decay, is represented by the spatial coordinates of the decay vertex. Unique to the KLOE experiment is the method of determining it by time measurement. It has been shown that for events in which the K_L decays into two neutral pions and the K_S decays into two charged ones, and where all the particles are detected, this procedure allows a determination of the K_L decay vertex with uncertainties of order 0.6 cm on the three coordinates [26]. Since in the events of interest for the present paper information is available only for two photons (instead of four), we have increased this uncertainty to 1 cm.

4.2 Analysis of the $K_L \to \pi^0 \pi^0$ background

We have generated two independent samples of events, consisting of 10^8 and 10^4 K_L's, respectively, out of which only those decaying inside the fiducial volume defined by the conditions $|z| < 150$ cm, and 40 cm$< R < 180$ cm were studied. For the first sample, K_L's were forced to proceed through the channel $K_L \to \pi^0 \pi^0$, while for the second through $K_L \to \pi^0 \nu \bar{\nu}$. We then determined the fraction of events for which two and only two photons were detected according to our simulation. These amount to 0.23% and 28% for the first and the second sample, respectively.

On this sample of events with only two detected photons we have made the following analyses:

1. We have studied the distribution of the reconstructed two–photon invariant mass, $M_{\gamma\gamma}^R$, after resolution effects are taken into account (Figure 2). In the $K_L \to \pi^0 \pi^0$ case more than 70% of the events are due to odd–pairings (i.e. the two photons come
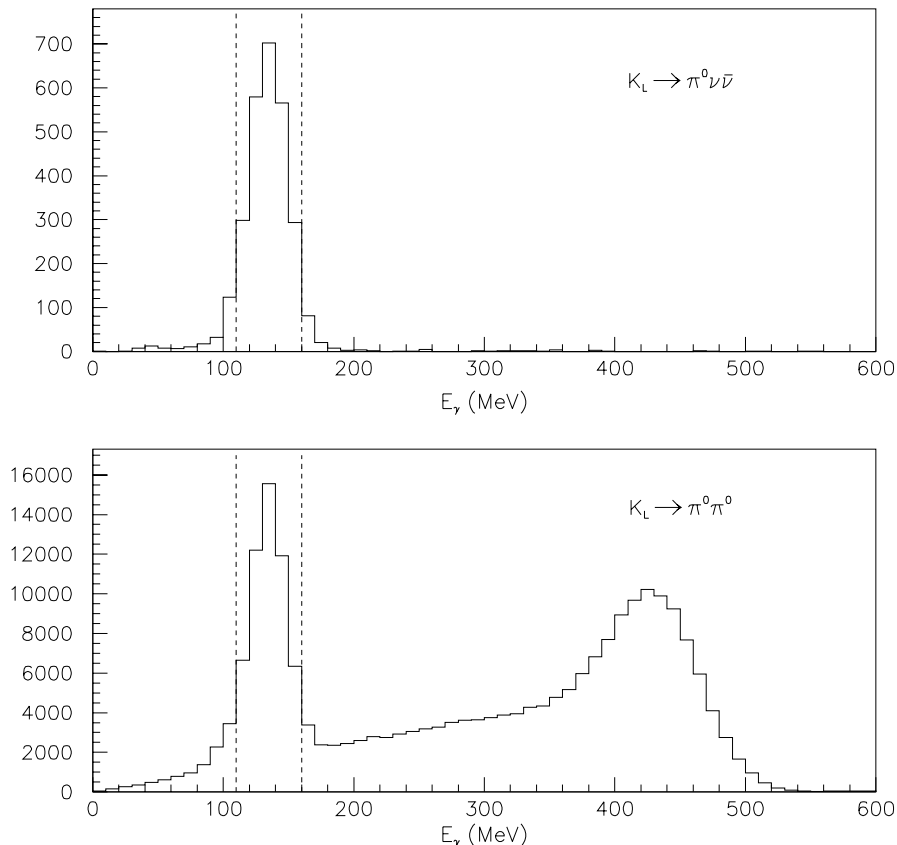
Figure 2: Two-photons invariant mass for events in which two and only two γ's are detected. Upper plot: $K_L \to \pi^0 \nu \bar{\nu}$ decays. Lower plot: $K_L \to \pi^0 \pi^0$ events. The dashed lines denote the mass window used in the analysis.

from two different π^0's), and can be easily removed by a cut on $M_{\gamma\gamma}^R$. Imposing $\left| M_{\gamma\gamma}^R - M_{\pi^0} \right| < 25$ MeV only 23% of the $K_L \to \pi^0 \pi^0$ background survives whereas the signal efficiency is 87%.

2. We then analyzed the distribution of the decay positions of the two samples, once the above cut on $M_{\gamma\gamma}^R$ is applied. Since the dead zones are not uniformly distributed inside the detector, the background distribution is expected to be peaked around the beam line. Figure 3 shows the amount of two photon events as a function of the decay radius, R_{decay}, for both signal and background. It can be seen that a cut on the minimum allowed decay radius can increase significantly the signal/background ratio, at the price of somewhat lowering the signal detection efficiency. For instance, by choosing events for which $R_{\text{min}} = 100$ cm $< R_{\text{decay}} < 180$ cm, gives a signal efficiency of 50% and reduces the background to 20%. The combined cuts on $M_{\gamma\gamma}^R$ and R_{min}, together with the two–photon requirement, leads to an overall background
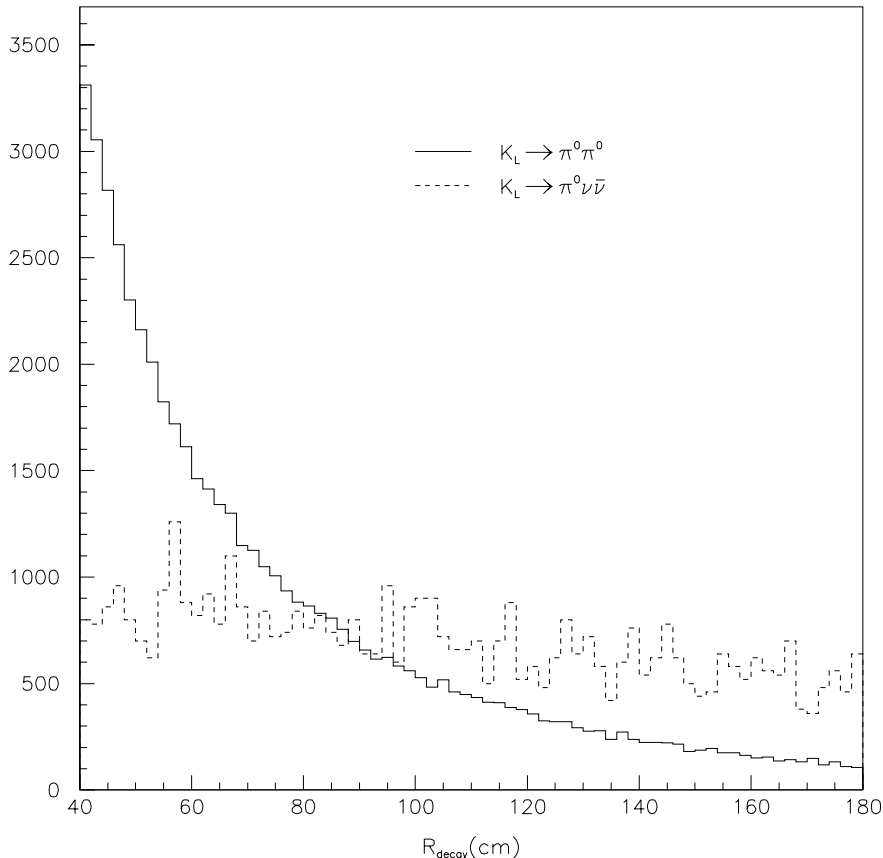
11

Figure 3: Decay radius for two-photons events from $K_L \to \pi^0 \nu \bar{\nu}$ (dashed line) and $K_L \to \pi^0 \pi^0$ (solid histogram) decays. As can be noticed, background events are concentrated mainly at positions close to the beam line. The two histograms are not on scale.

rejection of $\sim 10^{-4}$ and a 12% signal efficiency.

3. The use of the previously defined acceptance volume has the other advantage of providing a new powerful handle for background rejection. Since dead zones are concentrated *backwards* with respect to the K_L flight direction, momentum conservation implies that lost photons from $K_L \to \pi^0 \pi^0$ decays are mostly low energy ones in the laboratory frame. Consequently the distribution of the total reconstructed energy for two–photon events from $K_L \to \pi^0 \pi^0$ decays has to be displaced towards high values, as shown by Figure 4. Conversely, photons from signal events may have lower energies because a significant part of the total energy can be carried away by the two neutrinos. A cut around $E_{\text{tot}} = 0.22$ GeV leads to an additional 10^{-3} suppression of the $K_L \to \pi^0 \pi^0$ events.

The power of this method rests on two facts; firstly, one knows *a priori* what is the total available energy in the decay, since the K_L beam is monochromatic. Secondly,

12

as stated above, the detector's dead zone are concentrated in a well defined region with respect to the K_L flight direction (which in turn is determined by the ϕ decay angular distribution).

4. The other possible strategy for background rejection rests on the possibility of re-constructing the π^0 energy in the K_L rest frame ($E^*_{\pi^0}$). In this frame, π^0's from $K_L \to \pi^0\pi^0$ transitions are monochromatic with $E^*_{\pi^0} = M_{K^0}/2$, while for signal events $E^*_{\pi^0}$ ranges from M_{π^0} to $E^{\max}_\pi$ defined in (6). However, due to the finite de-tector's resolution, the two distributions overlap as shown in Figure 5. A cut around $E^*_{\pi^0} = 0.2$ GeV leads again to a 10^{-3} suppression of the residual $K_L \to \pi^0\pi^0$ events.

We have found that the two strategies, (i.e. cutting on E_{tot} or cutting on $E^*_{\pi^0}$) are very much correlated. Once either of the two cuts has been applied, the other is almost totally ineffective in decreasing the background. This can be understood since the detection of higher energy photons, which is an obvious requirement for the success of the first strat-egy, improves also the precision with which $E^*_{\pi^0}$ is reconstructed, since the ECAL energy resolution scales as $\sqrt{E}$. In other words, background events in the low–energy tails of both $E^*_{\pi^0}$ and E_{tot} distributions are strongly correlated. Furthermore, since the K_L momentum is small, it is also clear that the low E_{tot} region contains mainly signal events with small $E^*_{\pi^0}$.

4.3 Other background sources

Although the branching ratio of the $K_L \to 3\pi^0$ is $\sim$250 times larger than the $K_L \to \pi^0\pi^0$ one, the probability of detecting only one π^0 in the former kind of events is much sup-pressed with respect to the latter. Our Monte Carlo predicts a probability of about 10^{-8} of observing only two photons with 100 cm $< R_{\text{decay}} < 180$ cm from $K_L \to 3\pi^0$. We then estimate that applying the same cuts as in the $K_L \to \pi^0\pi^0$ case this background can be reduced to the level of about 10^{-10}.

A four–photon final state is produced also by the $K_L \to \pi^0\gamma\gamma$ transitions. However, the branching ratio of these events is a factor of ~ 500 lower than that of $K_L \to \pi^0\pi^0$. Moreover, of the four photons in the final state only two belong to a π^0, so that the cut on $M_{\gamma\gamma}$ is expected to work better than in the $K_L \to \pi^0\pi^0$ case. Since the rejection of the latter is at the 10^{-4} level before any cut E_{tot} or $E^*_{\pi^0}$, the $K_L \to \pi^0\gamma\gamma$ background does not represent a problem, at least for a search on $K_L \to \pi^0\nu\bar\nu$ above 10^{-10}.

Finally, all the K_L decays involving one π^0 and two charged particles should be easily rejected, since the KLOE drift chamber is able to detect with very high efficiency, within the fiducial volume, the presence of charged particles [27].
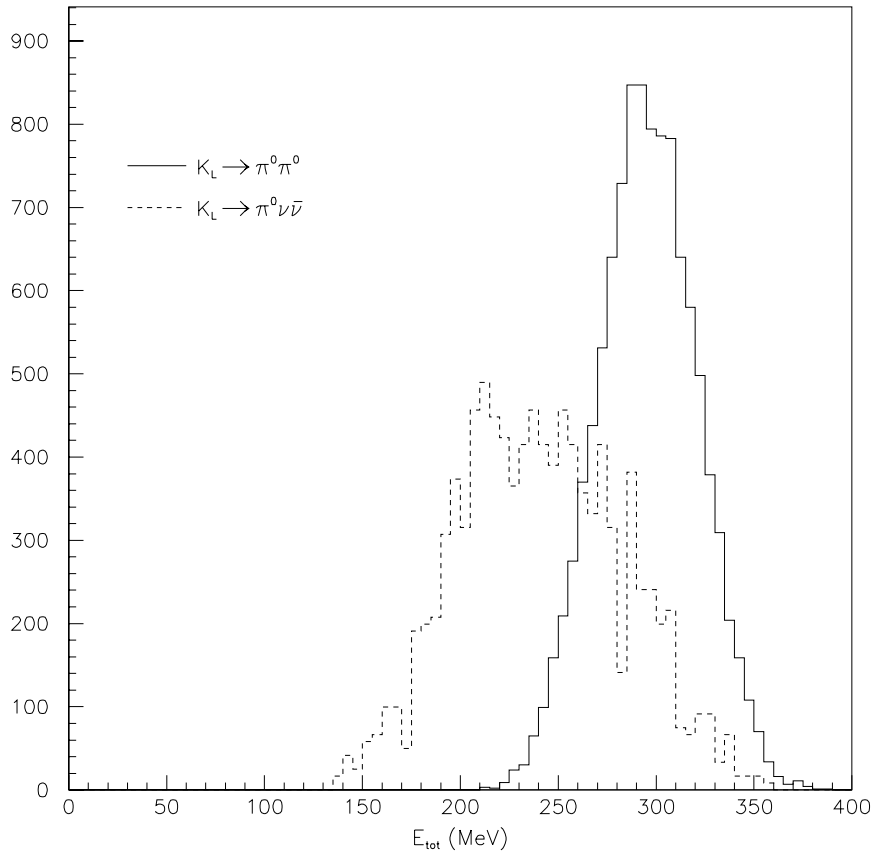
Figure 4: Total reconstructed energy for two-photons events from $K_L \to \pi^0 \nu \bar{\nu}$ (dashed line) and $K_L \to \pi^0 \pi^0$ (solid histogram) decays.

4.4 Discussion of the results

Table 1 summarizes our results. The case of KLOE and DAΦNE corresponds to the values in the upper part of the table. In the first two columns various combinations for the values of the cuts on E_{tot} (or $E_{\pi^0}^*$) and on $R_{\min}$, respectively, are listed. The efficiency obtained applying these cuts on signal events is shown in the third column. In the fourth column for any given set of cut values the Single Event Sensitivity (SES) is given, defined as the value of the $K_L \to \pi^0 \nu \bar{\nu}$ branching ratio for which the expected number of signal events equals that of background ones. Finally, in the last column, the value of the $K_L \to \pi^0 \nu \bar{\nu}$ branching ratio for which one event is expected after two years of data taking at the luminosity of 5×10^{32} cm^{-2}s^{-1} (BR1) is shown.

Note that there are two important effects which determine all the quoted signal efficiencies: the $\sim 67\%$ branching ratio of the $K_S \to \pi^+ \pi^-$ decay which is used for tagging purposes, and the fact that about 2/3 of the produced K_L's do not decay before reaching ECAL. Therefore, once a given set of cut values is chosen, the minimum obtainable value
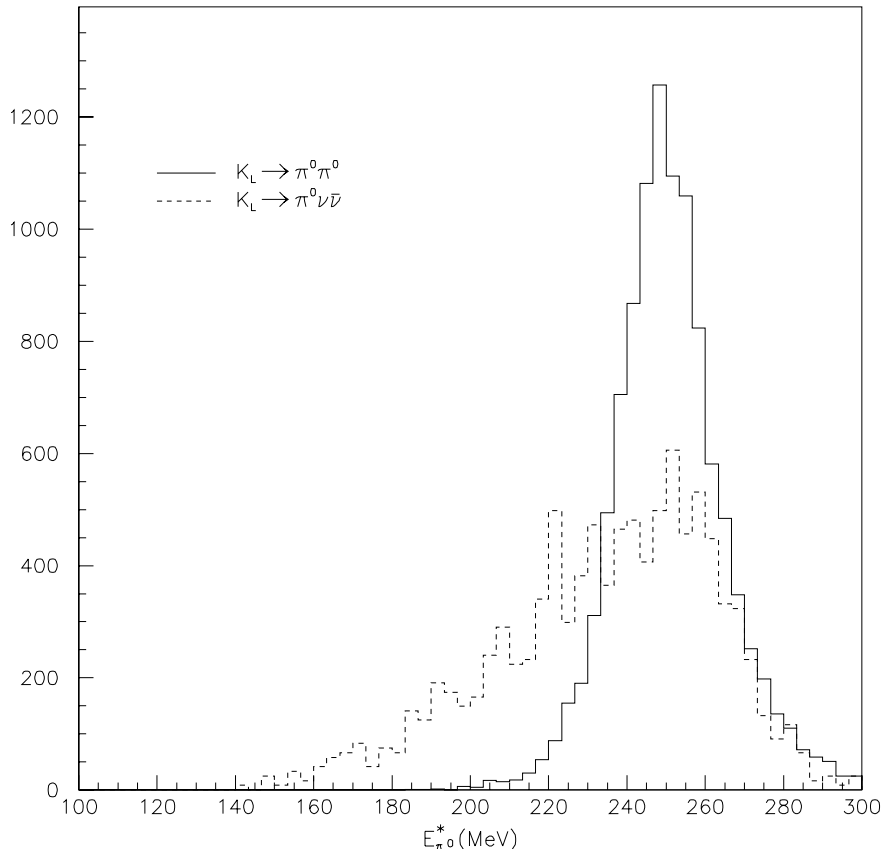
14

Figure 5: Reconstructed π^0 energy in the K_L rest frame for two-photon events from $K_L \rightarrow \pi^0\nu\bar{\nu}$ (dashed line) and $K_L \rightarrow \pi^0\pi^0$ (solid histogram) decays.

for BR1 is ultimately determined by the luminosity that can be delivered by the machine. In the case of DAΦNE one can hope to reach luminosities up to a factor ~ 2 larger than the nominal value, without modifying the hardware set–up of the machine. On the other hand, a good experiment should aim at reaching the minimum possible BR1, while keeping SES < BR1. A reasonable figure of merit for any given set of cut values is therefore the ratio R_{mer} =BR1/SES, which should be kept ≥ 1; it is seen that, in the case of KLOE, branching ratios of order 10^{-9} with figures of merit $R_{mer} \sim 1-2$ can be obtained, at best. This would already be a competitive measurement for several years to come.

Interestingly enough, there is not much space for possible improvements with the KLOE detector, since the benefits of a higher luminosity, which can decrease BR1, would be spoiled by the obtainable SES's, i.e. by the presence of an irreducible amount of background events. Although our analysis cannot be considered exhaustive and the possibility for a wiser and more effective strategy with KLOE and DAΦNE can always be considered, we believe that significant improvements on these figures can be obtained only by combining a more efficient detector with a higher luminosity accelerator. In particular,

15

	Energy cut (GeV)	R_{min}(cm)	ϵ(%)	SES	BR1
KLOE $\int \mathcal{L} = 10^{40}$ cm^{-2}	$E^*_{\pi^0} < 0.20$ $E_{\mathrm{tot}} < 0.22$ $E_{\mathrm{tot}} < 0.22$ $E_{\mathrm{tot}} < 0.21$	100 100 90 90	1.1 2.8 3.1 2.3	6×10^{-9} 1×10^{-9} 3×10^{-9} 5×10^{-10}	6×10^{-9} 2×10^{-9} 2×10^{-9} 3×10^{-9}
Ideal detector $\int \mathcal{L} = 10^{41}$ cm^{-2}	$E^*_{\pi^0} < 0.22$ $E_{\mathrm{tot}} < 0.24$ $E_{\mathrm{tot}} < 0.23$	100 100 100	2.8 5.7 4.1	$< 10^{-10}$ 1×10^{-10} $< 10^{-10}$	2×10^{-10} 1×10^{-10} 2×10^{-10}

Table 1: Efficiency, single event sensitivity (SES) and branching ratio of the signal that would yield one event (BR1) corresponding to different cuts in two typical situations: (1) the KLOE detector, with features as described in the text and for an integrated luminosity of 10^{40} cm^{-2}; (2) our definition of an ideal detector, with improved calorimeters as described in the text and for an integrated luminosity of 10^{41} cm^{-2}.

our simulation showed that the main problems of the present detector arise from losses of soft photons ($E < 50$ MeV) and from the spread in the energy resolution. For this reason, we have considered the possibility of one year of running at a luminosity of 1×10^{34} cm^{-2}s^{-1}, with a detector with the same geometry as KLOE but a better resolution, given by the following parameters: $\sigma_E = 2\% \times \sqrt{(E)}$ and 100% efficiency for photons with $E > 20$ MeV, both for QCAL and ECAL. It is seen that one not only improves in the reachable BR1 (thanks mainly to the higher luminosity), but also becomes more efficient in the rejection of the background, decreasing substantially the SES. Unfortunately, to our understanding, both the machine and the detector's parameters used in this case are not reachable in the next few years.

Figure 6 summarizes the physical information coming from an observation/search for both the neutral– and charged–kaon decay of interest here. On the two axes we have the two parameters r_K and θ_K (in fact the modulus of the sum of this phase plus the SM phase β), defined in Eq. (20). To each value of the two branching ratios $BR(K_L)$ and $BR(K^+)$ there corresponds a different curve in the $(r_K,\ \theta_K)$ plane, as shown in Fig. 6. A positive measurement of both branching ratios would allow one to pin down (modulo a two–fold ambiguity) the value of both parameters. Upper limits on the branching ratios only allow
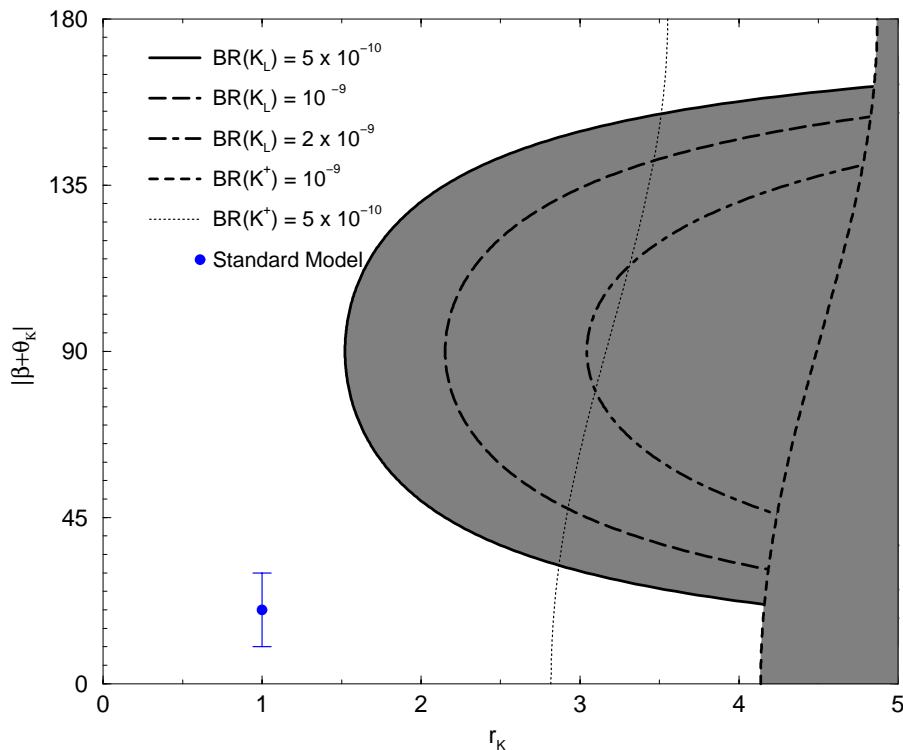
Figure 6: Combined information coming from limits/observations of $K_L \to \pi^0 \nu \bar{\nu}$ and $K^+ \to \pi^0 \nu \bar{\nu}$ around the 10^{-9} level. The parameters r_K and θ_K, describing New–Physics effects in the $s \to d\nu\bar{\nu}$ amplitude are defined in Eq. (20). The curves have been obtained assuming the central values of $|\lambda_{t,c}|$, X_{NL}^l and $X(m_i^2/M_W^2)$, as reported in [14]. The SM scenario is recovered for $r_K = 1$ and $\theta_K = 0$.

the exclusion of regions in that plane. The rightmost curve and shaded area on the figure correspond to the reference value of $BR(K^+) \leq 10^{-9}$, which is close to the current bound coming from the E787 experiment [12]. It is clear that the Standard Model value of the two parameters is far away from that curve, and that there is a very large region in parameter space to be explored. The curves corresponding to $BR(K_L) = (2, \ 1, \ 0.5) \times 10^{-9}$ show the possible improvements that a search for this decay in the following few years at a ϕ–factory could bring. In particular, the comparison to the curve corresponding to $BR(K^+) = 5 \times 10^{-10}$ shows very clearly that the two measurements/searches are complementary to each other: the $BR(K^+)$ $(BR(K_L))$ measurement strongly constrains the value of r_K (θ_K), leaving θ_K (r_K) practically undetermined. Even if $BR(K^+)$ was measured with rather small uncertainties, and found in agreement with the SM value, there would still be the possibility to have a *new–physics phase* θ_K very different from zero, and only the $BR(K_L)$ measurement could exclude this interesting scenario.

17

5 Conclusions

The observation of the $K_L \to \pi^0 \nu \bar{\nu}$ transition is of the utmost relevance, since it provides very clean information on one of the less known CKM matrix elements, and also because it could signal the presence of new physics beyond the Standard Model. The experimental challenge to perform such a measurement is a very difficult one, because of the very low expected branching ratio ($\sim 3 \times 10^{-11}$ in the Standard Model), and the presence of copious sources of background events which could fake the signal.

At present, there are three proposals for experiments which claim to be able to measure the SM branching ratio with a $\sim 10\%$ precision. None of these, however, will produce results for several years to come. On the other hand, we have seen that any measurement which can improve on the phenomenological limit 5×10^{-9} carries a non–trivial dynamical information on the structure of the $s \to d \nu \bar{\nu}$ amplitude, which at present is very poorly known, and would therefore constrain the parameter space of possible extensions of the SM.

We have argued that with the KLOE detector at DAΦNE it is possible to lower considerably the present experimental upper bound within a few years. Our main point is that the ϕ–factory environment is naturally well suited for the solution of the most difficult experimental problem, i.e. the rejection of the $K_L \to \pi^0 \pi^0$ background. Moreover, we have shown that the particular geometry of KLOE, a detector which was conceived and built to minimize the inefficiency in detecting photons, provides excellent possibilities to discriminate between signal and background events. With the present facility, one can reach a sensitivity to branching ratios of 10^{-9} or lower, in some years of running. This does not allow a positive observation of the Standard Model $K_L \to \pi^0 \nu \bar{\nu}$ transition: only a serious improvement in the delivered luminosity and in the detector's parameters would allow one to reach this ambitious goal. On the other hand Fig. 6 very clearly shows that KLOE has a chance to provide unique and invaluable information in excluding possible deviations from the SM in the value of the phase θ_K.

The results of the present paper are meant mainly as a preliminary and conservative estimate, only a dedicated detailed study on systematic effects could yield precise numbers on the sensitivity the KLOE detector could reach for such a decay. Our main aim was to show that this study is worthwhile and that an effort in this direction should be seriously taken into consideration. In this respect, we find it particularly relevant that this measurement does not require any modification in the data taking plans of KLOE. Moreover it is obvious that a detailed study of all the effects which may affect photon detection in KLOE is of the highest importance also with respect to ϵ'/ϵ studies, which are the main concerns of the Collaboration.

Acknowledgments

References

[1] S.L. Glashow, J. Iliopoulos and L. Maiani, Phys. Rev. **D2** (1970) 1285.

[2] M.K. Gaillard and B.W. Lee, Phys. Rev. Lett. **33** (1974) 108.

[3] L. Littenberg, Phys. Rev. **D39** (1989) 3322.

[4] G. Buchalla and A.J. Buras, Nucl. Phys. **B400** (1993) 225; Nucl. Phys. **B412** (1994) 106; Phys. Lett. **B333** (1994) 221.

[5] G. Buchalla and A.J. Buras, SLAC–PUB–7575, hep–ph/9707243.

[6] M. Lu and M. Wise, Phys. Lett. **B324** (1994) 461.

[7] W.J. Marciano and Z. Parsa, Phys. Rev. **D53** (1996) R1.

[8] Y. Grossman and Y. Nir, Phys. Lett. **B398** (1997) 163.

[9] G. Burdman, Phys. Lett. **B409** (1997) 443.

[10] Y. Nir and M.P. Worah, SLAC–PUB–7690, hep–ph/9711215.

[11] A.J. Buras, A. Romanino and L. Silvestrini, TUM–HEP–302/97, hep–ph/9712398.

[12] S. Adler *et al.* (E787 Collab.), BNL–64631, hep–ex/9708031.

[13] N. Cabibbo, Phys. Rev. Lett. **10** (1963) 531;
M. Kobayashi and T. Maskawa, Prog. Theor. Phys. **49** (1973) 652.

[14] G. Buchalla, A.J. Buras and M. Lautenbacher, Rev. Mod. Phys. **68** (1996) 1125;
A.J. Buras and R. Fleischer, hep–ph/9704376, to appear in "Heavy Flavours II", eds. A.J. Buras and M. Lindner (World Scientific, Singapore).

[15] M. Schmidtler and K.R. Schubert, Z. Phys. **C53** (1992) 347.

[16] A.J. Buras, M.E. Lautenbacher and G. Ostermaier, Phys. Rev. **D50** (1994) 3433.

[17] L. Wolfenstein, Phys. Rev. Lett. **51** (1983) 1945.

[18] C.Q. Geng, I.J. Hsu, Y.C. Lin, Phys. Lett. **B355** (1995) 569.

[19] Y. Grossmann, Y. Nir and M.P. Worah, Phys. Lett. **B407** (1997) 307,
see also Y. Grossmann, Y. Nir and R. Rattazzi, hep–ph/9701231, to appear in "Heavy Flavours II", eds. A.J. Buras and M. Lindner (World Scientific, Singapore).

[20] G. D'Ambrosio, G. Isidori and A. Pugliese, in "The Second DAΦNE Physics Handbook", Eds. L. Maiani, G. Pancheri and N. Paver (SIS–Frascati, 1995) p. 63 (hep–ph/9411389).

[21] M. Weaver *et al.*, Phys. Rev. Lett. **72** (191994) 3758.

[22] K. Arisaka *et al.*, hep–ex/9709026.

[23] T. Inagaki *et al.*, KEK–96/13 (1996).

[24] I.-H Chiang *et al.*, BNL–P926 (1996).

[25] The KLOE Collaboration, "A general Purpose detector for DAΦNE", LNF–92/019 (1992).

[26] The KLOE Collaboration, "The KLOE Detector, Technical Proposal", LNF–93/002 (1993).

[27] The KLOE Collaboration, "The KLOE Central Drift Chamber, Addendum to the Technical Proposal", LNF–94/028 (1994).

[28] The KLOE Collaboration, "The KLOE Data Acquisition System, Addendum to the Technical Proposal", LNF–95/014 (1995).

[29] The KLOE Collaboration, "The KLOE Trigger System, Addendum to the Technical Proposal", LNF–96/043 (1996).

[30] The KLOE Collaboration, "Status of the KLOE Experiment", LNF–97/033 (1997)

[31] Review of Particle Properties, Phys. Rev. **D54**, 1 (1996).

[32] M. Adinolfi *et al.*, "The QCAL calorimeter of KLOE", KLOE Internal–MEMO–063.

[33] The DAΦNE Project Team, "DAΦNE, Status and Plans", Proceedings of PAC95 (1995).